

## *Retraction*

# **Retracted: Prediction Mathematic Model and Influencing Factors of Contact Stress of Cylindrical Gear with Arc Tooth**

### **Complexity**

Received 19 December 2023; Accepted 19 December 2023; Published 20 December 2023

Copyright © 2023 Complexity. This is an open access article distributed under the Creative Commons Attribution License, which permits unrestricted use, distribution, and reproduction in any medium, provided the original work is properly cited.

This article has been retracted by Hindawi following an investigation undertaken by the publisher [1]. This investigation has uncovered evidence of one or more of the following indicators of systematic manipulation of the publication process:

- (1) Discrepancies in scope
- (2) Discrepancies in the description of the research reported
- (3) Discrepancies between the availability of data and the research described
- (4) Inappropriate citations
- (5) Incoherent, meaningless and/or irrelevant content included in the article
- (6) Manipulated or compromised peer review

The presence of these indicators undermines our confidence in the integrity of the article's content and we cannot, therefore, vouch for its reliability. Please note that this notice is intended solely to alert readers that the content of this article is unreliable. We have not investigated whether authors were aware of or involved in the systematic manipulation of the publication process.

Wiley and Hindawi regrets that the usual quality checks did not identify these issues before publication and have since put additional measures in place to safeguard research integrity.

We wish to credit our own Research Integrity and Research Publishing teams and anonymous and named external researchers and research integrity experts for contributing to this investigation.


The corresponding author, as the representative of all authors, has been given the opportunity to register their agreement or disagreement to this retraction. We have kept a record of any response received.

### **References**

- [1] Q. Zhang, G. Wen, S. Liang, Q. Tong, L. Hou, and G. Yang, "Prediction Mathematic Model and Influencing Factors of Contact Stress of Cylindrical Gear with Arc Tooth," *Complexity*, vol. 2020, Article ID 8888407, 15 pages, 2020.

## Research Article

# Prediction Mathematic Model and Influencing Factors of Contact Stress of Cylindrical Gear with Arc Tooth

Qi Zhang <sup>1,2</sup>, Guang Wen,<sup>2</sup> Shuang Liang,<sup>3</sup> Qin Tong,<sup>4</sup> Li Hou,<sup>3</sup> and Guangchun Yang<sup>1</sup>

<sup>1</sup>School of Intelligent Manufacturing, Panzhihua College, Panzhihua 617000, China

<sup>2</sup>Equipment Manufacturing College, Chengdu Industrial Vocational Technical College, Chengdu 610218, China

<sup>3</sup>School of Mechanical Engineering, Sichuan University, Chengdu 610065, China

<sup>4</sup>School of Mechanical and Electrical Engineering, Mianyang Normal University, Mianyang 621000, China

Correspondence should be addressed to Qi Zhang; pzhuzq@stu.scu.edu.cn

Received 26 August 2020; Revised 3 October 2020; Accepted 12 October 2020; Published 3 November 2020

Academic Editor: Zhihan Lv

Copyright © 2020 Qi Zhang et al. This is an open access article distributed under the Creative Commons Attribution License, which permits unrestricted use, distribution, and reproduction in any medium, provided the original work is properly cited.

Given the absence of a theoretical formula to analyze the influence of parameters on the contact stress of cylindrical gear with arc tooth, an explicit mathematical model of cylindrical gear with arc tooth between the design parameters and the contact stress is established based on Kriging surrogate model. The parameters of the variation function of Kriging model are optimized by using the whale optimization algorithm (WOA), and the explicit mathematical model accuracy between the design parameters and the contact stress of the gear is in turn optimized by the improved Kriging surrogate model. The influence of design parameters on the contact stress of cylindrical gear with arc tooth is analyzed based on the established mathematical model. The proposed algorithm was realized via the programming platform MATLAB; the simulation results indicate that the precision evaluation indexes (the correlation coefficient ( $R^2$ ), root mean square error (RMSE), and the relative maximum absolute error (RMAE)) of the proposed Kriging model are improved, in addition to the error range which is narrowed from  $(-2, 4)$  to  $(0, 3)$ . As the tooth width, modulus, pressure angle, and tooth line radius increased, the contact stress of the cylindrical gear with arc tooth gear declined, which was negatively correlated with the design parameter. The amplitude of contact stress of the cylindrical gear with arc tooth was the largest due to the change of tooth radius, followed by the change of modulus, while the influence of tooth width was less. Finally, the influence of modulus-tooth line radius interaction and pressure angle-tooth line radius interaction on contact stress of cylindrical gear with arc tooth was significant.

## 1. Introduction

Gears are widely used in various industries [1], and the involute cylindrical gear is widely used at present. However, in the involute cylindrical gear, the bearing capacity of spur gear is limited, the axial force of helical gear subsists, and the processing technology of herringbone gear is complex. In order to solve the problem of involute gear, Japanese scholar Yoshiro Hasegawa and others put forward a new type of circular arc gear transmission device. This new type of gear transmission has the advantages of good meshing performance, high coincidence, no axial force, stable transmission, and so on [2]. For this kind of gear, scholars have carried out in-depth research. Tseng et al. have studied its mathematical model, undercutting conditions, contact, and other aspect

[3–6]. Lei et al. have studied the accurate three-dimensional modeling method of circular tooth profile gear [7]. Dengqiu et al. have studied its contact distribution [8]. The contact performance of gears was studied by Chen Shuai and Wang [9, 10, 11, 12]. Surrogate model is an approximate modeling method that can generate mathematical models with a small number of samples to reduce the number of physical experiments and improve efficiency, and the commonly used surrogate model mainly includes response surface, Kriging, Support Vector Machine, Artificial Neural Network, etc. [13, 14]. In order to study the influence of design parameters on the contact stress of circular arc tooth line gear, this paper proposes using Kriging surrogate model to establish the mathematical model of contact stress between design parameters (tooth width, modulus, pressure angle, and tooth

radius) of cylindrical gear with arc tooth. The Kriging model with the best effect is selected by comparing the prediction effect of these common surrogate model methods on contact stress of cylindrical gear with arc tooth. With a view to improving the modeling accuracy of Kriging model, intelligent algorithm is used to optimize the variation function of Kriging; the commonly used intelligent algorithm mainly includes genetic algorithm, immune algorithm, simulated annealing algorithm, particle swarm algorithm, fish swarm algorithm, ant colony algorithm, cuckoo algorithm, and so forth [15]. In this paper, whale optimization algorithm (WOA) was used for the parameters of the variation function of the traditional Kriging model. The Kriging surrogate model with optimized parameters of the variation function is used to establish the explicit mathematical model between the design parameters and the contact stress of the gear. The influence of design parameters (tooth width, modulus, pressure angle, and tooth radius) on the contact stress of circular arc tooth line cylindrical gear is discussed based on the established mathematical model.

## 2. Mathematical Model of Circular Arc Gear

According to its forming principle [16, 17], the coordinate system of forming principle of circular arc tooth line cylindrical gear is shown in Figure 1. In Figure 1,  $S(O - XYZ)$  is the static coordinate system,  $S_1(O_1 - X_1Y_1Z_1)$  is the solidification coordinate of the gear blank, and  $S_T(O_T - X_TY_TZ_T)$  is the tool coordinate, which moves in relation to  $S(O - XYZ)$  coordinate at the speed of  $V_T = R \times \omega$ .

In the coordinate system  $S_T(O_T - X_TY_TZ_T)$ , the vector expression of the parametric equation of the surface formed in the cutting process is

$$\begin{aligned} \vec{r}_T = & -\left(\frac{\pm q \sin \alpha + R_T \pm \pi m}{4}\right) \cos \theta \vec{i}_T \\ & + \left(\frac{\pm q \sin \alpha + R_T \pm \pi m}{4}\right) \sin \theta \vec{j}_T + q \cos \alpha \vec{k}_T, \end{aligned} \quad (1)$$

$$\begin{cases} \vec{r}_{dq} = \pm \sin \alpha \cos \theta \vec{i}_T \pm \sin \alpha \sin \theta \vec{j}_T + \cos \alpha \vec{k}_T, \\ \vec{r}_{d\theta} = -\left(\frac{\pm q \sin \alpha + R_T + \pi m}{4}\right) \sin \theta \vec{i}_T + \left(\frac{\pm q \sin \alpha + R_T + \pi m}{4}\right) \cos \theta \vec{j}_T. \end{cases} \quad (4)$$

Then, the unit normal vector of the tool surface is

$$\begin{aligned} \vec{n} = \frac{\vec{r}_{dq} \times \vec{r}_{d\theta}}{|\vec{r}_{dq} \times \vec{r}_{d\theta}|} = & -\cos \alpha \cos \theta \vec{i}_T - \cos \alpha \sin \theta \vec{j}_T \\ & \pm \sin \alpha \vec{k}_T. \end{aligned} \quad (5)$$

where  $a$  is the pressure angle of the cutting edge of the cutting tool;  $\theta$  is the angle from the current enveloping point of the gear blank to the middle section; and  $q$  is the length of the enveloping reference point from the point on the cutting surface of the cutting tool along the direction of the generatrix of the cutting cone in the coordinate system.  $R$  is dividing circle radius of gear,  $R_T$  is cutter head radius of machining tool,  $R_n$  is inner edge radius in the tangent direction of dividing circle,  $R_w$  is outer edge radius in the tangent direction of dividing circle,  $R_w = R_T + \pi m/4$ ,  $m$  is gear module,  $\omega$  is cutter head rotation angle speed of machining tool, and  $V_T$  is cutter head moving speed of machining tool.

Transform  $S_T(O_T - X_TY_TZ_T)$  to  $S(O - XYZ)$ , and its coordinate conversion relationship is as follows:

$$\mathbf{T}_{OT} = \begin{bmatrix} 1 & 0 & 0 & R\varphi + R_T \\ 0 & 0 & 1 & R \\ 0 & 1 & 0 & 0 \\ 0 & 0 & 0 & 1 \end{bmatrix}. \quad (2)$$

Transform  $S(O - XYZ)$  to  $S_1(O_1 - X_1Y_1Z_1)$ , and its coordinate conversion relationship is

$$\mathbf{T}_{10} = \begin{bmatrix} \cos \varphi & -\sin \varphi & 0 & 0 \\ \sin \varphi & \cos \varphi & 0 & 0 \\ 0 & 0 & 1 & 0 \\ 0 & 0 & 0 & 1 \end{bmatrix}. \quad (3)$$

If  $S_T(O_T - X_TY_TZ_T)$  is converted to  $S(O - XYZ)$ , then the coordinate transformation matrix is  $\mathbf{T}_{1T} = \mathbf{T}_{10} \mathbf{T}_{OT}$ .

**2.1. Unit Normal Vector of Tool Surface.** The tool surface equation is

**2.2. Relative Speed of Tool and Gear at Meshing Point.** The direction vector can be expressed as

$$\vec{\lambda} = \overline{O_1O_T} = (R\varphi + R_T) \vec{i}_T + R \vec{k}_T. \quad (6)$$

Therefore, the relative speed of the tool and the gear at the meshing point is

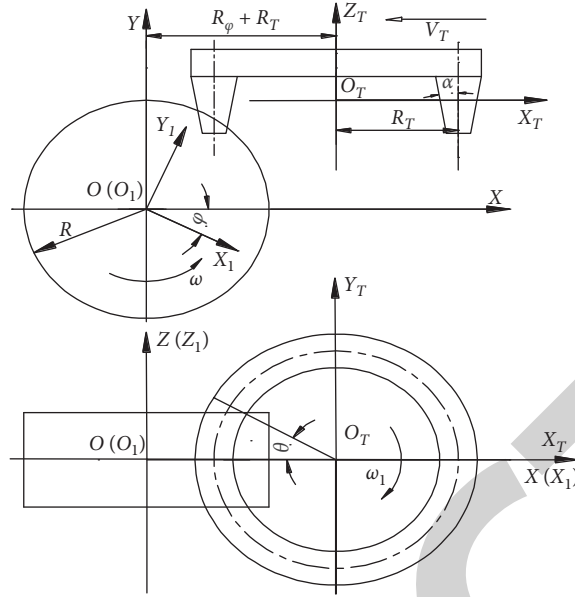


FIGURE 1: Coordinate system of forming principle of cylindrical gear with arc tooth.

$$\begin{aligned}
 \vec{v}^{12} &= \vec{\omega}^{12} \times \vec{r}^1 + \frac{d\lambda}{dt} - \vec{\omega}^2 \times \vec{\lambda}, \\
 &= -\omega_1 q \cos \alpha \vec{i}_T - \omega_1 \left( \frac{\pm q \sin \alpha + R_T + \pi m}{4} \right) \cos \theta \vec{k}_T + \omega_1 R \vec{i}_T \\
 &\quad - \left[ \omega_1 R \vec{i}_T - \omega_1 (R\phi + R_T) \vec{k}_T \right], \\
 &= -q \cos \alpha \omega_1 \vec{i}_T - \left[ \left( \frac{\pm q \sin \alpha + R_T + \pi m}{4} \right) \cos \theta + (R\phi + R_T) \right] \omega_1 \vec{k}_T.
 \end{aligned} \tag{7}$$

2.3. *Meshing Function.* Based on the meshing principle, the meshing function is expressed as follows:

$$\Gamma = \vec{n} \cdot \vec{v}^{12} = 0. \tag{8}$$

Because  $\omega_1 \neq 0$ , it can be concluded from the above formula that

$$q = \mp \sin \alpha \frac{\cos \theta (R_T + \pi m/4) + (R\phi + R_T)}{\cos \theta}. \tag{9}$$

2.4. *Conjugate Surfaces.* Combining equations (1) and (9), the contact line equation between the tool and the gear to be machined is as follows:

$$\begin{cases}
 x_T = -\left( \frac{\pm q \sin \alpha + R_T \pm \pi m}{4} \right) \cos \theta, \\
 y_T = \left( \frac{\pm q \sin \alpha + R_T \pm \pi m}{4} \right) \sin \theta, \\
 z_T = q \cos \alpha, \\
 q = \mp \sin \alpha \frac{\cos \theta (R_T + \pi m/4) + (R\phi + R_T)}{\cos \theta}.
 \end{cases} \tag{10}$$

By converting the coordinates in  $S_T(O_T - X_T Y_T Z_T)$  to  $S_1(O_1 - X_1 Y_1 Z_1)$ , the tooth surface equation of the cut gear can be obtained as follows:

$$\left\{ \begin{array}{l} x_1 = \left[ -\left( \frac{\pm q \sin \alpha + R_T \pm \pi m}{4} \right) \cos \theta + R\varphi + R_T \right] \cos \varphi - (q \cos \alpha + R) \sin \varphi, \\ y_1 = \left[ -\left( \frac{\pm q \sin \alpha + R_T \pm \pi m}{4} \right) \cos \theta + R\varphi + R_T \right] \sin \varphi + (q \cos \alpha + R) \cos \varphi, \\ z_1 = \left( \frac{\pm q \sin \alpha + R_T \pm \pi m}{4} \right) \sin \theta, \\ q = \mp \sin \alpha \frac{\cos \theta (R_T + \pi m/4) + (R\varphi + R_T)}{\cos \theta}. \end{array} \right. \quad (11)$$

2.5. *Instantaneous Contact Line.* Meshing function  $\Gamma = \Gamma(q, \theta, \varphi)$  is a function of variables  $q, \theta, \varphi$ . As  $\varphi_1 = \omega_1 t$ ,  $\varphi_1$  is regarded as a function of entering  $\Gamma$  in a certain instant, thus the function expression of the instantaneous contact line between the rack cutter and the gear blank can be obtained. If the value  $\varphi_1$  at any time is substituted into equation (7), the contact line equation of the whole surface can be obtained as follows:

$$\left\{ \begin{array}{l} x_T = -\left[ (1 + \sin^2 \alpha) \left( \frac{R_T \pm \pi m}{4} \right) + \sin^2 \alpha \frac{R\varphi + R_T}{\cos \theta} \right] \cos \theta, \\ y_T = \left[ (1 + \sin^2 \alpha) \left( \frac{R_T \pm \pi m}{4} \right) + \sin^2 \alpha \frac{R\varphi + R_T}{\cos \theta} \right] \sin \theta, \\ z_T = \mp \sin \alpha \cos \alpha \left( \left( \frac{R_T \pm \pi m}{4} \right) + \left( \frac{R\varphi + R_T}{\cos \theta} \right) \right). \end{array} \right. \quad (12)$$

2.6. *Tooth Profile Equation.* In the axial middle section of the gear, from its extended coordinate system, it can be seen that  $b=0$ ; then,  $\theta$  is also equal to zero. Substituting these two parameters into equation (11), the tooth profile equation of the middle section is obtained:

$$\left\{ \begin{array}{l} x_1 = \left[ -\left( \frac{\pm q \sin \alpha + R_T \pm \pi m}{4} \right) + R\varphi + R_T \right] \cos \varphi - (q \cos \alpha + R) \sin \varphi, \\ y_1 = \left[ -\left( \frac{\pm q \sin \alpha + R_T \pm \pi m}{4} \right) + R\varphi + R_T \right] \sin \varphi + (q \cos \alpha + R) \cos \varphi, \\ q = \mp \sin \alpha \left( \left( \frac{R_T + \pi m}{4} \right) + R\varphi + R_T \right). \end{array} \right. \quad (13)$$

According to equation (13), it can be seen that the tooth profile of the axial symmetry surface of the gear is involute.

Similarly, on the axial asymmetric plane, let  $z_1 = b$ ; according to the expressions of  $Z_1$  and  $q$  in equation (11), we can get

$$\varphi = \frac{\{ [(-b/\tan \theta) + (R_T \pm \pi m/4) \cos \theta] / \sin^2 \alpha - (R_T \pm \pi m/4) \cos \theta - R_T \}}{R} \quad (14)$$

Thus, the expression of the tooth profile of the non-intermediate section can be obtained as follows:

$$\left\{ \begin{array}{l} x_T = \left[ -\left( \frac{\pm q \sin \alpha + R_T \pm \pi m}{4} \right) \cos \theta + R\varphi + R_T \right] \cos \varphi - (q \cos \alpha + R) \sin \varphi, \\ y_T = \left[ -\left( \frac{\pm q \sin \alpha + R_T \pm \pi m}{4} \right) \cos \theta + R\varphi + R_T \right] \sin \varphi + (q \cos \alpha + R) \cos \varphi, \\ q = \mp \sin \alpha \frac{\cos \theta (R_T + \pi m/4) + (R\varphi + R_T)}{\cos \theta}, \\ \varphi = \frac{\{[-(b/\tan \theta) + (R_T \pm \pi m/4) \cos \theta] / \sin^2 \alpha - (R_T \pm \pi m/4) \cos \theta - R_T\}}{R}. \end{array} \right. \quad (15)$$

### 3. Contact Stress Analysis of Cylindrical Gear with Arc Tooth Based on Finite Element Method

**3.1. Model Material Attribute Definition.** Establish material information in ABAQUS, such as modulus of elasticity ( $E=2.08$  MPa), Poisson's ratio (0.298), and other parameters.

**3.2. Establishing Analytical Steps and Interactions.** Establish analysis steps, which mainly include defining analysis type (static), defining analysis increment step, determining iteration method, creating field variable, and historical variable and determining output parameters. Turn on nonlinearity, and define interaction as contact; then set contact type of finite element analysis of circular arc tooth line gear pair as "friction free." The MPC (multipoint constraint) is established by the rotating centers of the active and the driven.

**3.3. Applying Restraint and Moment.** The torque of magnitude  $6.08 \times 10^4$  N-mm is applied to the driving wheel. At the same time, MPC is added to the driving wheel: the direction of its rotation axis is set as free, and other rotation and translation are set as fixed. In the driven wheel, all directions of MPC constraints are fixed, and no motion is allowed in any direction.

**3.4. Gridding.** The method of sweeping is used to divide the mesh of gear pair, with C3D8I as the mesh type. The overall unit size of the gear is set to 2 mm, while the local subdivision size of the contact area is 0.02 mm. If the requirements are not met, continue to adjust the parameters. In the subsequent calculation, the mesh can be further refined to improve the quality of division. Through multiple trial calculation and comparative analysis results, the grid can be used as the final analysis grid if the calculation result is nearly stable. In the analysis process, due to the local subdivision of

the contact area, the number of grids for each pair of gears is about  $1.2 \times 10^6$ . The result of gear grid division is shown in Figure 2.

**3.5. Solution and Visualization.** Considering that the mesh number of each pair of gears is about  $1.2 \times 10^6$ , a parallel calculation is used in the solution. The calculated stress nephogram of driving wheel and that of driven wheel are shown in Figure 3. Figure 3(a) shows the dynamic contact stress diagram of driving wheel, and Figure 3(b) shows the contact stress diagram of driving wheel.

According to the simulation analysis, contact area is near dividing circle. As shown in Figure 3(a), the driving wheel of the contact area of the above standard pitch circle has a maximum stress value of 503.3 MPa. As shown in Figure 3(b), driven wheel contact area of the below standard pitch circle has a maximum stress value of 501 MPa. Therefore, the maximum contact stress is 503.3 MPa, and the difference in value between active and driven wheel is 2.3 MPa, only equal to 0.4570% of the maximum contact stress, which almost can be ignored. Similarly, it can be seen from Figures 3(a) and 3(b) that the contact area of the gear studied in this paper is an ellipse under the action of load, which confirms the fact that the contact area of point contact gear under the action of load is ellipse.

### 4. The Prediction Model of Contact Stress of Cylindrical Gear with Arc Tooth Based on Surrogate Model

**4.1. Test Design and Response Results.** The common test methods mainly include uniform test design, orthogonal test design, Latin square test design, and other methods. This paper studies the relationship between tooth width, modulus, pressure angle, tooth radius, and contact force. Four factors and three levels are selected for the simulation scheme by using the principle of regression orthogonal test method. The level table of gear design factors is shown in Table 1.

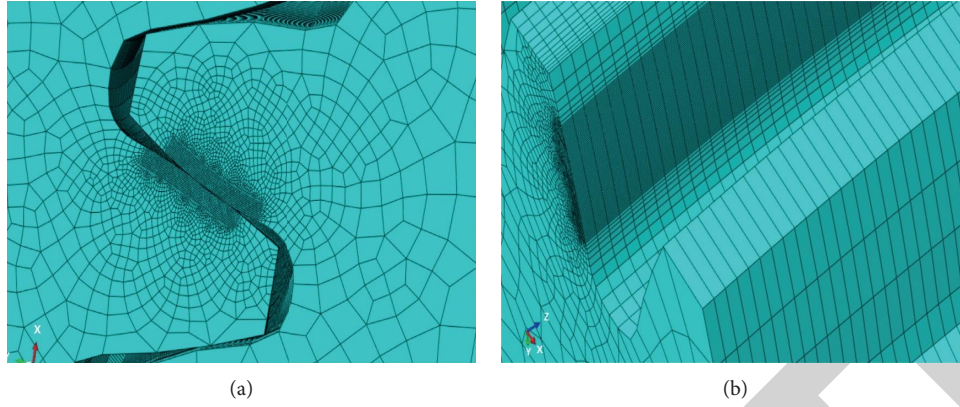


FIGURE 2: Meshing results of gears. (a) Global mesh results. (b) Local mesh results.

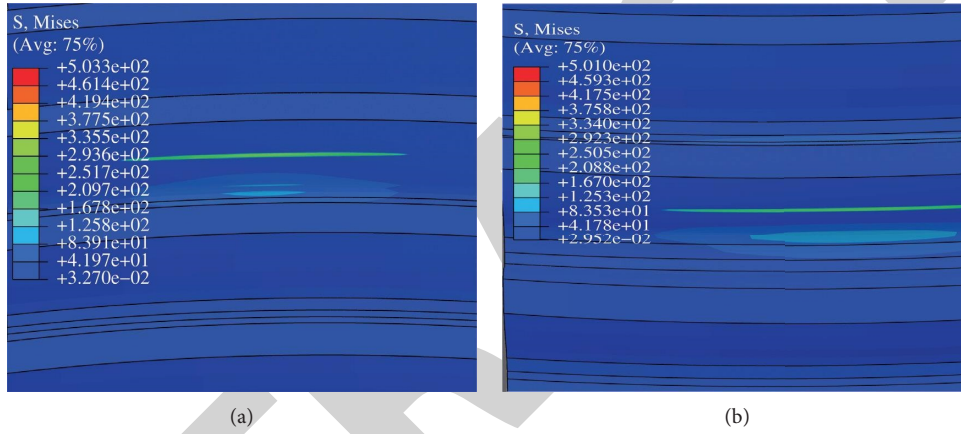


FIGURE 3: Stress neutrogram analysis of driving wheel and driven wheel. (a) Driving wheel. (b) Driven wheel.

TABLE 1: Gear design factor level.

| Level order | Tooth width (mm) | Modulus | Pressure angle (°) | Tooth radius (mm) |
|-------------|------------------|---------|--------------------|-------------------|
| Level 1     | 38.83685         | 2.96737 | 18.83685           | 191.8425          |
| Level 2     | 40               | 3.2     | 20                 | 250               |
| Level 3     | 41.16315         | 3.43263 | 21.16315           | 308.1575          |

In this paper, the orthogonal test is used to sample, and then the finite element method is used to get the gear joint stress under different sample data. According to the orthogonal table, 9 samples were processed, and the contact stress simulation results of  $L9$  (34) orthogonal test arc gear are shown in Table 2.

#### 4.2. Improved Kriging Model

**4.2.1. Kriging Surrogate Model.** Kriging model can obtain ideal fitting results when solving the problem of high nonlinearity. Its interpolation results are defined as the linear weighting of the response value of the known sample function, which is

$$y(x) = \sum_{j=1}^k \beta_j f_j(x) + Z(x). \quad (16)$$

In the formula,  $f_j(x)$  is function,  $\beta_j$  is corresponding coefficient, and  $Z(x)$  is static random process, whose mean value is 0, and its variance is  $\sigma^2$ . The covariance between the random variables corresponding to two different points in the design space is

$$\text{Cov}[Z(x^i), Z(x^j)] = \sigma^2 R(x^i, x^j), \quad (17)$$

$$R(x^i, x^j) = \prod_{l=1}^{N_s} R_l(\theta_l, x_l^i, x_l^j), \quad (18)$$

TABLE 2: Contact stress simulation results of L9 (34) orthogonal test.

| Order | Tooth width (mm) | Modulus | Pressure angle (°) | Tooth radius (mm) | Contact force (MPa) |
|-------|------------------|---------|--------------------|-------------------|---------------------|
| 1     | 38.83685         | 2.96737 | 18.83685           | 191.8425          | 542.7               |
| 2     | 38.83685         | 3.2     | 20                 | 250               | 457.2               |
| 3     | 38.83685         | 3.43263 | 21.16315           | 308.1575          | 396.8               |
| 4     | 40               | 2.96737 | 20                 | 308.1575          | 452.9               |
| 5     | 40               | 3.2     | 21.16315           | 191.8425          | 494.1               |
| 6     | 40               | 3.43263 | 18.83685           | 250               | 449.1               |
| 7     | 41.16315         | 2.96737 | 21.16315           | 250               | 469.6               |
| 8     | 41.16315         | 3.2     | 18.83685           | 308.1575          | 440.2               |
| 9     | 41.16315         | 3.43263 | 20                 | 191.8425          | 476.7               |

where  $R(x^i, x^j)$  is correlation function, which represents the correlation between random variables at different positions. The commonly used correlation function is Gaussian-type function.

In equation (17), the parameter  $\theta$  of the variation function of Kriging model is determined by the maximum likelihood estimation method to solve the optimization problem:

$$\max \left\{ -\frac{N_s}{2} \ln(\hat{\sigma}^2) - \frac{1}{2} \ln(R) - \frac{N_s}{2} \ln(2\pi) \right\}, \quad \theta > 0, \quad (19)$$

$$\hat{\sigma}^2 = \frac{1}{N_s} (y_s - F\tilde{\beta})^T R^{-1} (y_s - F\tilde{\beta}).$$

In order to minimize the root mean square error (RMSE) between Kriging prediction value and actual function value, the approximate expression of Kriging model can be obtained as

$$\tilde{y}(x) = f_x^T \tilde{\beta} + \left[ R(x, x^{(1)}), R(x, x^{(2)}), \dots, R(x, x^{(N_s)}) \right]^T R^{-1} (y_s - F\tilde{\beta}), \quad (20)$$

where  $F$  is matrix composed of basis function vector  $f_x^T$ ;  $\tilde{\beta}$  is least square estimate of KRG model coefficient;  $R$  is correlation matrix; and  $N_s$  is sample number.

**4.2.2. Whale Algorithm.** The principle of whale algorithm is derived from the "bubble net" foraging behavior of humpback whales. The mathematical expression based on this special strategy is as follows:

$$D = |C \cdot X^*(t) - X(t)|, \quad (21)$$

$$X(t+1) = X^*(t) - A \cdot D,$$

where  $t$  is the number of current iterations;  $X(t)$  is the coordinate vector of the current humpback whale;  $X(t+1)$  is the target coordinate vector after the next iteration;  $X^*(t)$  is the best position vector obtained so far, which is updated with time;  $D$  is the distance between the current humpback whale and the best position; and  $A$  and  $C$  are the number of systems, which are, respectively, expressed as

$$A = 2a \cdot r - a, \quad (22)$$

$$C = 2r,$$

where  $a$  is parameter in the value range (0, 2) and linearly decreasing with the iteration time and  $r$  is random vector in the interval (0, 1).

When  $|A| > 1$ , whales have the behavior of wandering and foraging. Using the random individual coordinates of the population to locate and navigate food, the mathematical expression is as follows:

$$X(t+1) = X_{\text{rand}}(t) - A \cdot D. \quad (23)$$

When  $|A| < 1$ , there were two behaviors of encircling and attacking prey, and the mathematical model is described as follows:

$$X(t+1) = X^*(t) - D \cdot e^{bl} \cdot \cos(2\pi l). \quad (24)$$

In the formula,  $b$  is the constant of the spiral shape and  $l$  is the random number on the interval  $(-1, 1)$ .

Since the contraction and spiral position updating of whales are carried out synchronously, mathematically selecting the same way of probability to update their position, then we can get the following expression:

$$X(t+1) = \begin{cases} X^*(t) - A \cdot D, & p < 0.5, \\ X^*(t) - D \cdot e^{bl} \cdot \cos(2\pi l), & p \geq 0.5. \end{cases} \quad (25)$$

According to the characteristics of Kriging and WOA algorithm, the Kriging surrogate model based on WOA algorithm is used for parameter impact analysis, and the flow chart is shown in Figure 4.

**4.3. Accuracy Evaluation Indexes of Kriging.** Generally, the evaluation indexes of correlation coefficient ( $R^2$ ), root mean square error (RMSE), and relative maximum absolute error (RMAE) are used to evaluate the accuracy of Kriging.

**4.3.1. The Correlation Coefficient ( $R^2$ ).**

$$R^2 = 1 - \frac{\sum_{i=1}^n (f_i - \hat{f}_i)^2}{\sum_{i=1}^n (f_i - \bar{f})^2}. \quad (26)$$

**4.3.2. The Root Mean Square Error (RMSE).**

$$\text{RMSE} = \sqrt{\frac{\sum_{i=1}^n (f_i - \hat{f}_i)^2}{n}}. \quad (27)$$



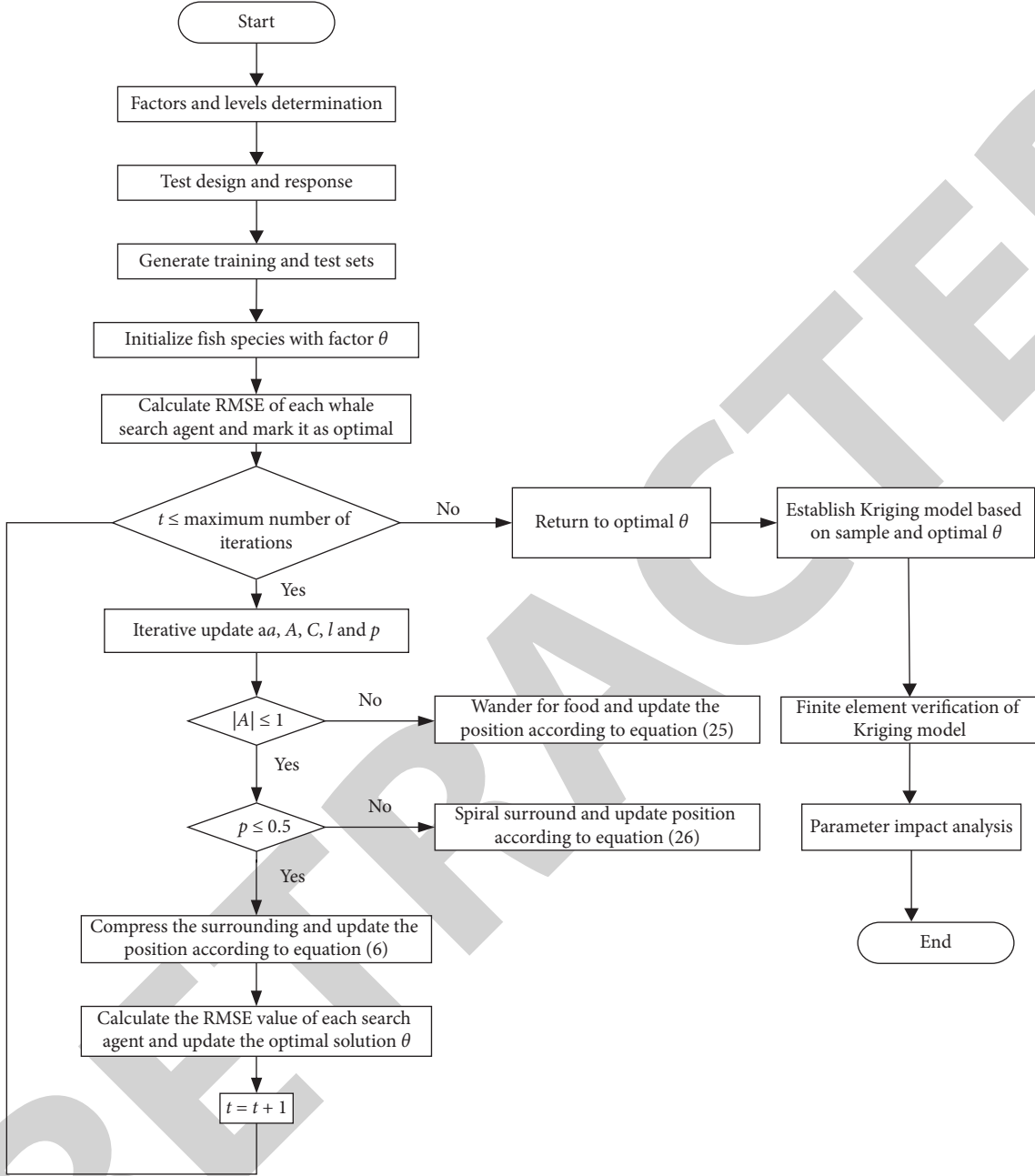


FIGURE 4: Improvement process of Kriging surrogate model based on WOA algorithm.

#### 4.3.3. The Relative Maximum Absolute Error (RMAE).

$$\text{RMAE} = \frac{\max\{|f_1 - \hat{f}_1|, |f_2 - \hat{f}_2|, \dots, |f_n - \hat{f}_n|\}}{\sqrt{1/n} \sum_{i=1}^n (f_i - \bar{f})^2}. \quad (28)$$

In equations (26) to (28),  $n$  is number of test sample points,  $f_i$  is the truth value of the actual model at the  $i^{\text{th}}$  test sample point, and  $\hat{f}_i$  is the predicted value of the surrogate model at the  $i^{\text{th}}$  test sample point. The closer  $R^2$  is to 1, the better the global approximation effect of the surrogate model will be. The smaller the RMSE is, the higher the precision of the surrogate

model will be, and the smaller the RMAE is, indicating that the higher the precision of the surrogate model will be.

4.4. Numerical Simulation. Using the MATLAB digital simulation platform, Kriging and the improved Kriging algorithm based on WOA algorithm are, respectively, used to establish the contact stress prediction model of circular arc gear. The evaluation indexes of the correlation coefficient ( $R^2$ ), root mean square error (RMSE), and the relative maximum absolute error (RMAE) before and after optimization are shown in Table 3.

TABLE 3: Evaluation indexes before and after optimization.

| Indexes | Kriging | WOA-Kriging | Optimization effect (%) |
|---------|---------|-------------|-------------------------|
| $R^2$   | 0.9922  | 0.9974      | 0.52                    |
| RMSE    | 2.8569  | 1.6540      | 42.11                   |
| RMAE    | 0.1322  | 0.0754      | 42.97                   |

It can be seen from Table 3 that the correlation coefficient ( $R^2$ ) has increased from 0.9922 to 0.9974, which is 0.52% higher and closer to 1. The correlation coefficient is closer to 1 implying that the global approximation ability of the optimized Kriging model is better. RMSE is used to indicate the impairment between the estimated value and the actual value. The higher the value of RMSE, the greater the impairment. After optimization, RMSE went from 2.8569 to 1.6540, reducing by 42.11%, which shows that the optimized Kriging model can better estimate the samples. After optimization, RMAE decreased from 0.1322 to 0.0754, which is 42.97% lower and closer to 0. This shows that the local error is less after optimization. Therefore, Kriging algorithm is improved based on WOA algorithm, which enhances the fitting ability and accuracy of Kriging algorithm.

The residual graph histogram of the test set for the contact stress prediction model is established by using Kriging and the improved Kriging algorithm based on WOA, as shown in Figures 5(a) and 5(b).

It can be seen from Figure 5 that the error dispersion of the optimized Kriging based on the improved WOA to establish the contact stress prediction model of the circular arc gear is more centralized, and the optimized error range is reduced from  $(-2, 4)$  to  $(0, 3)$ , which significantly improved accuracy.

**4.5. Finite Element Verification.** In order to further verify the validity of the established mathematical model, the finite element method is used to analyze the gear. The definition of material attribute of the model, the establishment of analysis steps and interactions, the application of constraints and moments, and mesh division are the same as those in Section 3. The gear parameters are shown in Table 4, and the results of the finite element analysis are shown in Figure 6.

As shown in Figure 6, the maximum contact stress of the gear is 472.2 MPa. The mathematical model established in Section 4.3 is used to predict the maximum contact stress of the gear in Table 4.

As shown in Table 5, the mathematical model established in Section 4.3 is used to predict the maximum contact stress of gears in Table 4. Compared with the results of finite element analysis, the maximum error is 3.2013 MPa, which shows that the mathematical model can effectively predict the contact stress of gears.

## 5. Influence of Design Parameters on Contact Stress

In this section, the influence of design parameters on contact stress is discussed based on the explicitly mathematical model between the gear design parameters (tooth width,

modulus, pressure angle, and tooth line radius) and the contact stress of cylindrical gear with arc tooth by using the proposed WOA-Kriging model. When the parameters (tooth width, modulus, pressure angle, and tooth line radius) are changed separately, the influence of tooth width, modulus, pressure angle, and tooth line radius on the contact stress of cylindrical gear with arc tooth is shown in Figure 7.

As seen in Figure 7, with the increase of tooth width, modulus, pressure angle, and tooth line radius, the contact stress of the cylindrical gear with arc tooth gear was in decline, which was negatively correlated with the design parameter, the amplitude of contact stress of the cylindrical gear with arc tooth is the largest due to the change of tooth radius, followed by the change of modulus, and the influence of tooth width is less.

The influence of change in tooth width, modulus, pressure angle, and tooth line radius on contact stress of the cylindrical gear with arc tooth is shown in Figure 8.

As seen in Figure 8, when tooth width interacts with modulus, pressure angle, and tooth line radius, respectively, the variation range of contact stress for the cylindrical gear with arc tooth gear is in decline. The response surface is not large and the complexity of surface is not high, indicating that the influence of tooth width interacting with modulus, pressure angle, and tooth line radius, respectively, on the contact stress is not significant. When modulus interacts with modulus, pressure angle, and tooth line radius, respectively, the complexity of the stress response surface is relatively high, which indicates that the influence on the stress is significant, compared with tooth width interacting with modulus, pressure angle, and tooth line radius, respectively. When pressure angle interacts with tooth line radius, the complexity of the stress response surface is relatively high, which also indicates that the influence on the stress is significant. Influence of modulus-tooth line radius interaction on contact stress of cylindrical gear with arc tooth and influence of pressure angle-tooth line radius interaction on contact stress of cylindrical gear with arc tooth are significant. In the contour map above, the smaller the distance between the contour lines is, the greater the influence of their interaction on the contact stress will be.

## 6. Conclusion

In order to study the influence of design parameters of cylindrical gear with arc tooth on its contact stress, a mathematical model of tooth width, modulus, pressure angle, radius of tooth line, and contact stress of gear is established by using Kriging surrogate model. Meanwhile,

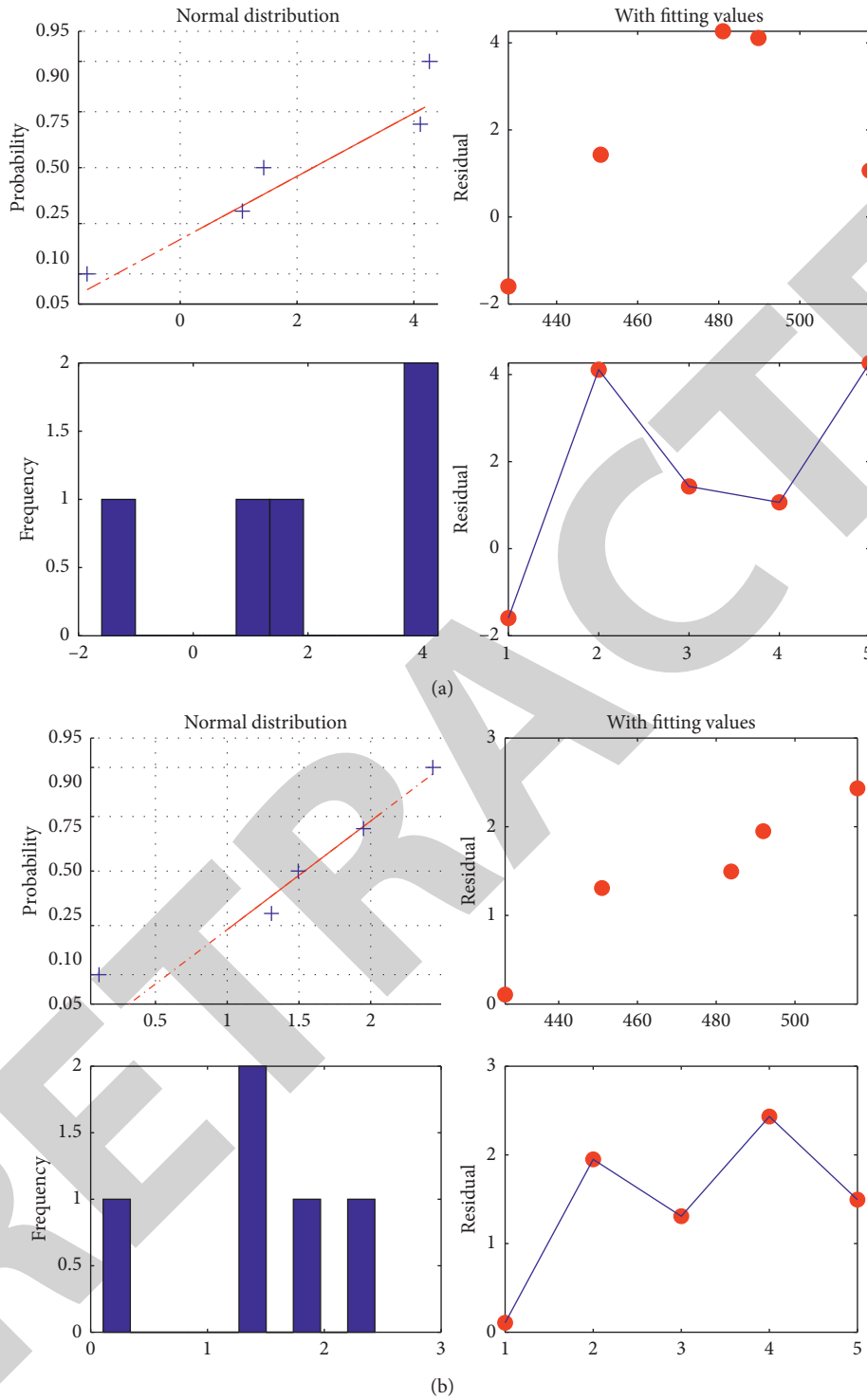


FIGURE 5: Residual diagram of contact stress prediction model. (a) Residual diagram of contact stress prediction model based on Kriging ((A) residual histogram, (B) residual with sequence, (C) residual, (D) sequence of observations). (b) Residual diagram of contact stress prediction model based on Kriging based on WOA ((A) residual histogram, (B) residual with sequence, (C) residual, (D) sequence of observations).

a Kriging model modeling method based on the whale optimization algorithm (WOA) is proposed. The parameters of variation function of traditional Kriging model are optimized by whale optimization calculation to improve the modeling accuracy of Kriging model. Based

on the established mathematical model, the influence of design parameters (tooth width, module, pressure angle, and tooth radius) of cylindrical gear with arc tooth on the contact stress of circular arc tooth line cylindrical gear is discussed.

TABLE 4: Gear parameters of finite element analysis.

| Order | Tooth width (mm) | Modulus  | Pressure angle (°) | Tooth radius (mm) |
|-------|------------------|----------|--------------------|-------------------|
| 1     | 38.836850        | 3.2      | 20                 | 308.157500        |
| 2     | 38.836850        | 2.967370 | 18.836850          | 308.157500        |
| 3     | 40               | 3.432630 | 21.163150          | 308.157500        |
| 4     | 40               | 3.432630 | 20.000000          | 191.842500        |
| 5     | 40               | 2.967370 | 21.163150          | 250               |

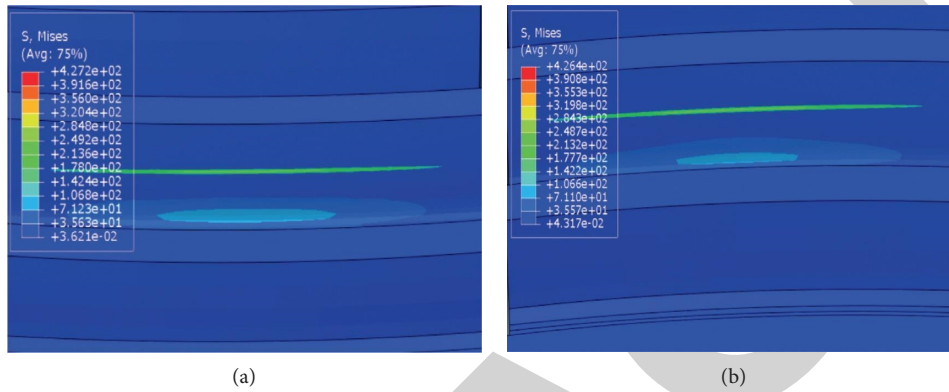


FIGURE 6: Stress nephogram of driving wheel and driven wheel. (a) Driving wheel. (b) Driven wheel.

TABLE 5: Finite element prediction results.

| Order | Tooth width (mm) | Modulus  | Pressure angle (°) | Tooth radius (mm) | Finite element stress (MPa) | Predicted stress (MPa) | Error (MPa) |
|-------|------------------|----------|--------------------|-------------------|-----------------------------|------------------------|-------------|
| 1     | 38.83685         | 3.2      | 20                 | 308.157500        | 427.2                       | 429.7935               | 2.5935      |
| 2     | 38.83685         | 2.967370 | 18.836850          | 308.157500        | 462.3                       | 465.5013               | 3.2013      |
| 3     | 40               | 3.432630 | 21.163150          | 308.157500        | 396.4                       | 394.7222               | -1.6778     |
| 4     | 40               | 3.432630 | 20.000000          | 191.842500        | 479.2                       | 478.3456               | -0.8544     |
| 5     | 40               | 2.967370 | 21.163150          | 250               | 470                         | 471.8039               | 1.8039      |

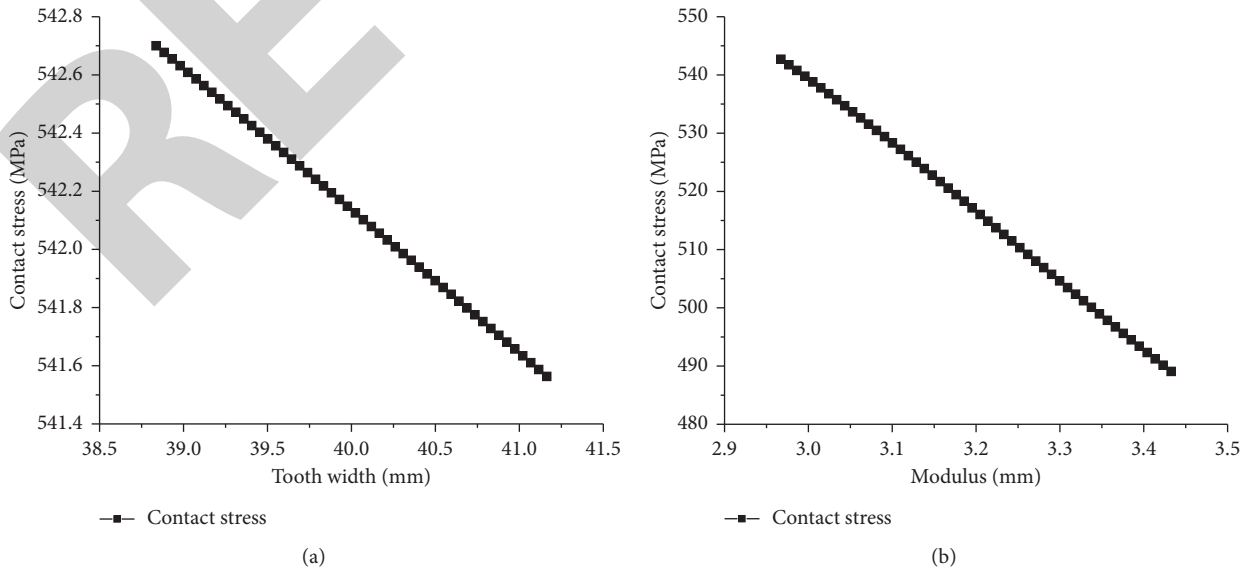


FIGURE 7: Continued.

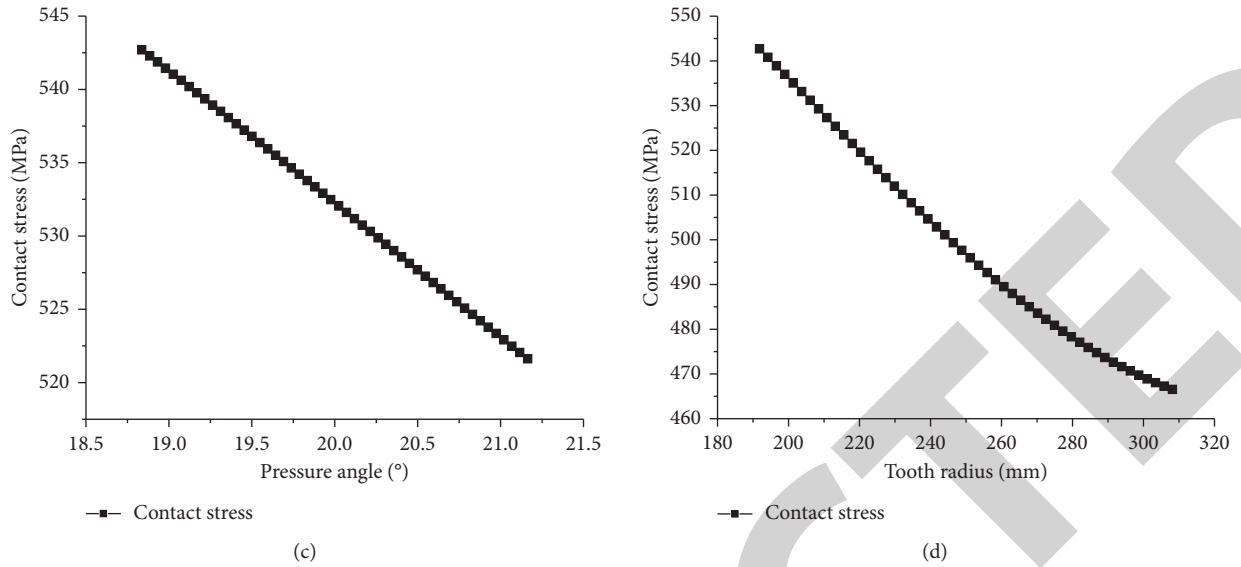
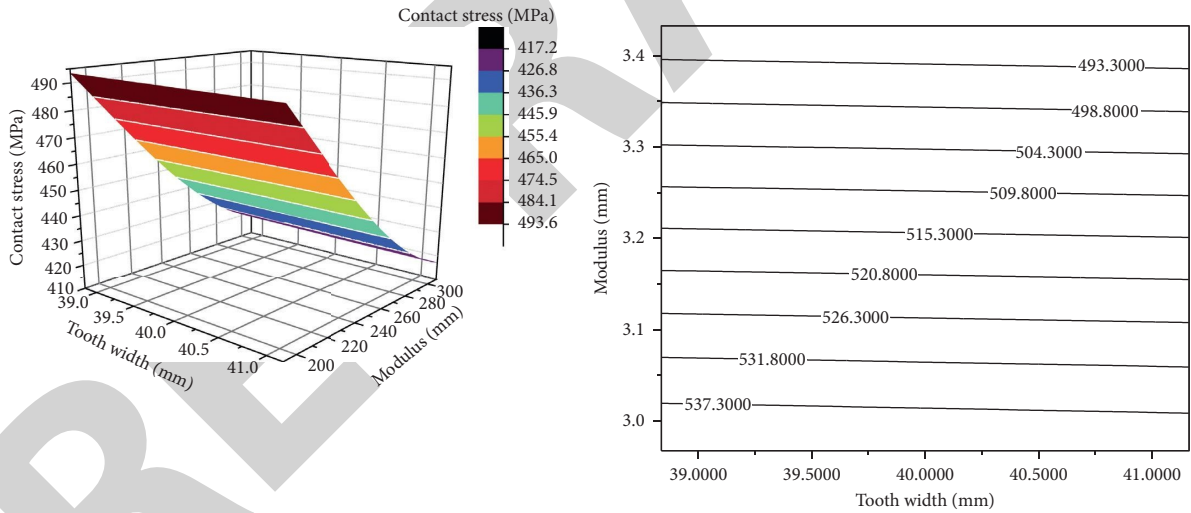
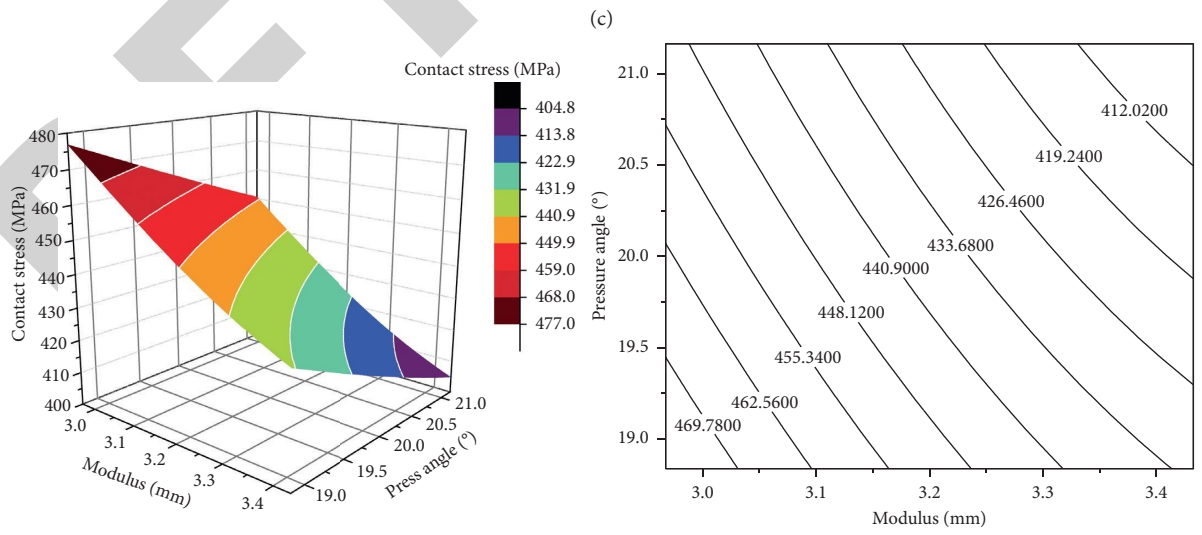
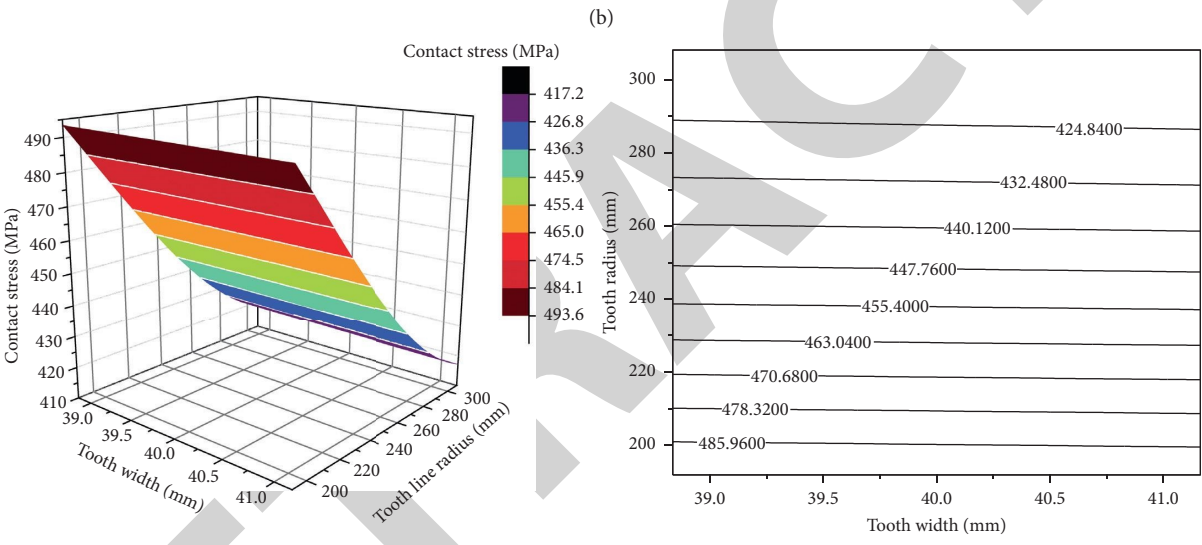
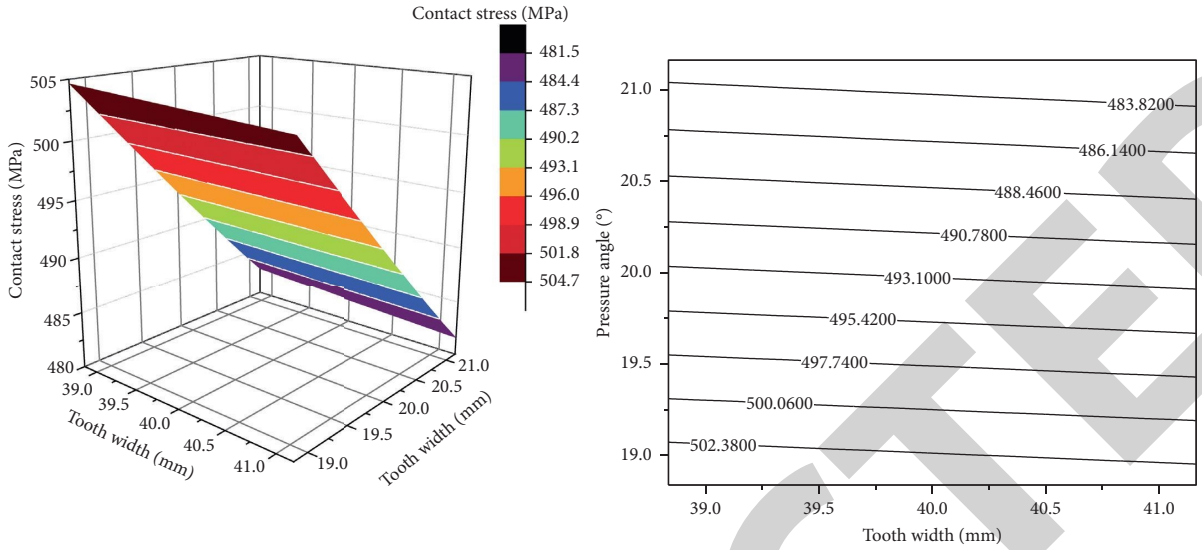


FIGURE 7: Influence of design parameters on contact stress. (a) Influence of tooth width on contact stress contact stress of cylindrical gear with arc tooth. (b) Influence of modulus on contact stress contact stress of cylindrical gear with arc tooth. (c) Influence of pressure angle on contact stress contact stress of cylindrical gear with arc tooth. (d) Influence of tooth line radius on contact stress contact stress of cylindrical gear with arc tooth.



(a) FIGURE 8: Continued.



(d)  
FIGURE 8: Continued.

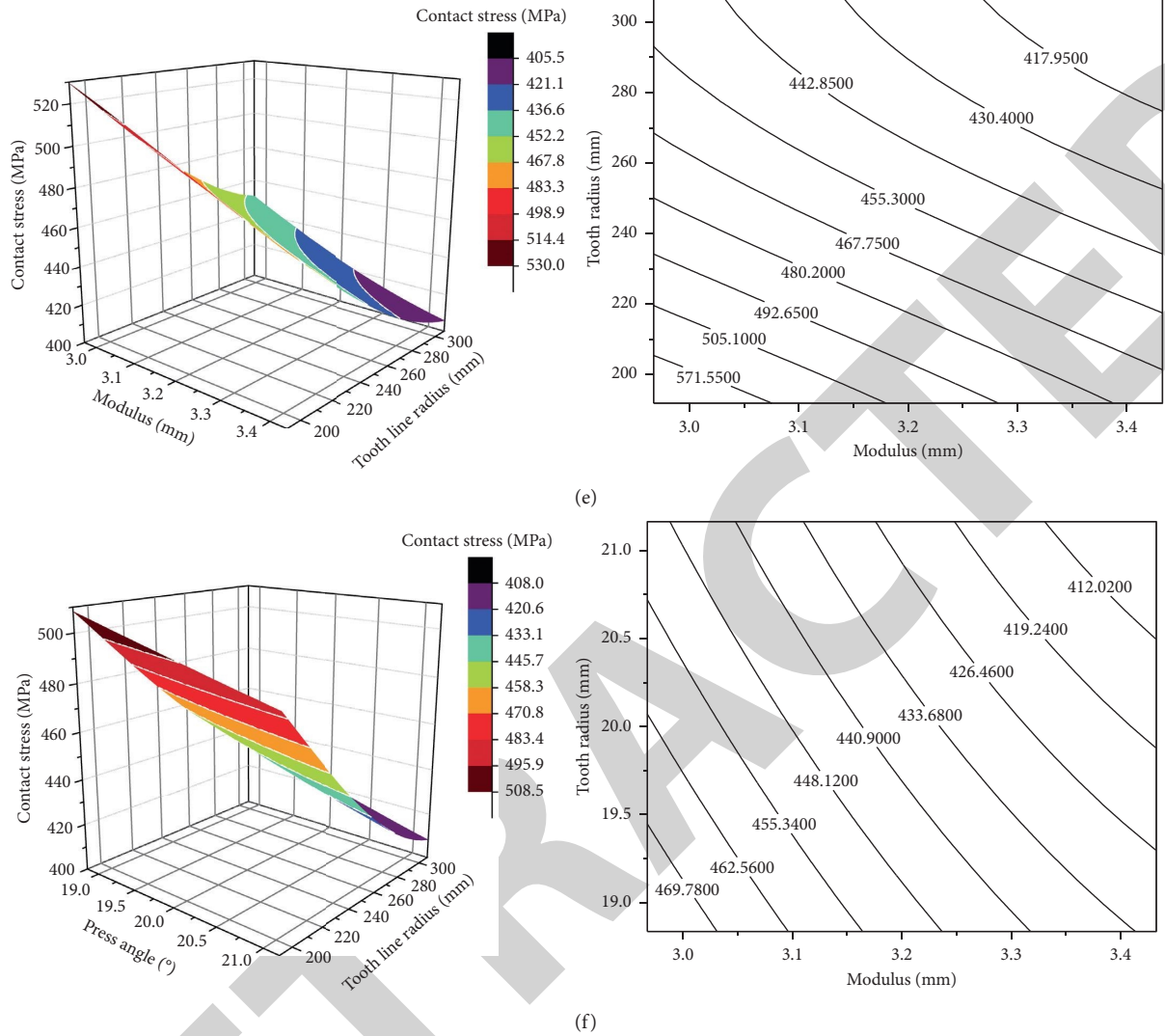


FIGURE 8: Influence of design parameters interaction on contact stress of cylindrical gear with arc tooth. (a) Influence of tooth width-modulus interaction on contact stress of cylindrical gear with arc tooth. (b) Influence of tooth width-pressure angle interaction on contact stress of cylindrical gear with arc tooth. (c) Influence of tooth width-tooth line radius interaction on contact stress of cylindrical gear with arc tooth. (d) Influence of modulus-pressure angle interaction on contact stress of cylindrical gear with arc tooth. (e) Influence of modulus-tooth line radius interaction on contact stress of cylindrical gear with arc tooth. (f) Influence of pressure angle-tooth line radius interaction on contact stress of cylindrical gear with arc tooth.

- (1) Based on the improved Kriging model of WOA algorithm, the correlation coefficient ( $R^2$ ) is increased from 0.9922 to 0.9974, MSE is reduced from 2.8569 to 1.6540, and RMAE is also reduced from 0.1322 to 0.0754. The correlation coefficient ( $R^2$ ) of the improved algorithm is improved, and root mean square error (RMSE) and relative maximum absolute error (RMAE) are improved to some extent, which improves the global approximation ability of the traditional Kriging algorithm, reduces the local error, and improves the fitting accuracy.
- (2) Both the traditional Kriging algorithm and the improved Kriging algorithm based on WOA algorithm can establish the contact stress prediction model of gear, and the accuracy is within the applicable range.

The error range of Kriging is  $(-2, 4)$ , while the error range of Kriging algorithm based on WOA algorithm is  $(0, 3)$ . The accuracy of the improved Kriging has been optimized obviously, and the accuracy of the model is verified by the finite element method, where the maximum error is only 2.5935 MPa.

- (3) Based on the established mathematical model, the influence of design parameters (tooth width, modulus, pressure angle, and tooth radius) on the contact stress of circular arc tooth line cylindrical gear is discussed. With the increase of tooth width, modulus, pressure angle, and tooth line radius, the contact stress of the cylindrical gear with arc tooth gear was in decline, which was negatively correlated with the design parameter, the amplitude of contact

stress of the cylindrical gear with arc tooth is the largest due to the change of tooth radius, followed by the change of modulus, and the influence of tooth width is the least. And influence of modulus-tooth line radius interaction and pressure angle-tooth line radius interaction on contact stress of cylindrical gear with arc tooth is significant.

## Data Availability

The data used to support the findings of this study are available from the corresponding author upon request.

## Conflicts of Interest

The authors declare that they have no known conflicts of interest or personal relationships that could have appeared to influence the work reported in this paper.

## Acknowledgments

This project was supported by National Natural Science Foundation of China (nos. 51875370 and 51375320), by Science and Technology Research Program of Sichuan Province (no.2018JY0420), by the seed fund of University Science Park of Panzhuhua City (no. University Science Park 2019-25), and by University Key Laboratory of Sichuan in Process Equipment and Control Engineering (GK201905).

## References

- [1] J. Li, Q. J. Sun, and L. Q. Wang, "Tooth contact analysis of involute gear," *Chinese Journal of Engineering Design*, vol. 16, no. 1, pp. 27–31, 2009.
- [2] S. Hasegawa, "Cutting machine of cylindrical gears with curvilinear shaped teeth," *Precision Machine*, vol. 18, no. 8, pp. 253–257, 1952.
- [3] J. T. Tseng and C. B. Tsay, "Mathematical model and surface deviation of cylindrical gears with curvilinear shaped teeth cut by a hob cutter," *Journal of Mechanical Design*, vol. 127, no. 5, pp. 982–987, 2005.
- [4] R.-T. Tseng and C.-B. Tsay, "Contact characteristics of cylindrical gears with curvilinear shaped teeth," *Mechanism and Machine Theory*, vol. 39, no. 9, pp. 905–919, 2004.
- [5] J.-T. Tseng and C.-B. Tsay, "Undercutting and contact characteristics of cylindrical gears with curvilinear shaped teeth generated by hobbing," *Journal of Mechanical Design*, vol. 128, no. 3, pp. 634–643, 2006.
- [6] A. Fuentes, R. Ruiz-Orzaez, and I. Gonzalez-Perez, "Computerized design, simulation of meshing, and finite element analysis of two types of geometry of curvilinear cylindrical gears," *Computer Methods in Applied Mechanics and Engineering*, vol. 272, pp. 321–339, 2014.
- [7] C. Lei, H. Li, Z. Fei et al., "Accurate three-dimensional modeling of cylindrical gear with variable hyperbolic circular-arc-tooth-trace," *Machinery Design & Manufacture*, vol. S1, pp. 54–56, 2019.
- [8] D. Dengqiu, Y. Zhenhuan, F. Qianjun, and A. Yu, "Research on contact stress distribution and meshing position change rule of variable hyperbolic cylindrical gear with arcuate tooth trace," *Design and Research*, vol. 9, pp. 53–58, 2019.
- [9] C. Shuai, H. Li, T. Meng et al., "Dynamic contact characteristic analysis of cylindrical gear with variational hyperbola and circular-arc-tooth-trace," *Journal of Mechanical Transmission*, vol. 42, no. 9, pp. 85–89, 2018.
- [10] W. Hong, H. Li, Z. Fei, H. Lin-Tong, Z. Qi-Fan, and Q. Xin, "Dynamic contact analysis of cylindrical gear with arcuate tooth trace," *Modular Machine Tool & Automatic Manufacturing Technique*, vol. 6, pp. 37–40, 2017.
- [11] Z. Haiyan, H. Li, W. Yongqiao, H. Linli, and L. Bo, "Modeling and contact strength analysis for modified cylindrical gear profile with arcuate tooth trace," *Journal of Mechanical Transmission*, vol. 39, no. 7, pp. 20–22, 2015.
- [12] L. Bo, H. Li, J. Ping et al., "Modeling and contact strength analysis of cylindrical gear with arcuate tooth trace," *Journal of Mechanical Transmission*, vol. 38, no. 2, pp. 100–105, 2014.
- [13] A. K. Gupta, "Predictive modelling of turning operations using response surface methodology, artificial neural networks and support vector regression," *International Journal of Production Research*, vol. 48, no. 3-4, pp. 763–778, 2010.
- [14] B. Gaspar, A. P. Teixeira, and C. G. Soares, "Assessment of the efficiency of kriging surrogate models for structural reliability analysis," *Probabilistic Engineering Mechanics*, vol. 37, pp. 24–34, 2014.
- [15] V. I. Skoullis, I. X. Tassopoulos, and G. N. Beligiannis, "Solving the high school timetabling problem using a hybrid cat swarm optimization based algorithm," *Applied Soft Computing*, vol. 52, pp. 277–289, 2016.
- [16] L. Qin, L. Haidong, and Z. Qi, "Study on the tooth surface equation and parametric modeling for new type of cylindrical gear with arc tooth trace," *Journal of Mechanical Transmission*, vol. 40, no. 8, pp. 50–53, 2016.
- [17] D. Fayun and Z. Qi, "Mathematical model and modal analysis of new type of circular arc tooth trace cylindrical gear," *Journal of Mechanical Transmission*, vol. 42, no. 1, pp. 22–26, 2018.